Journal of Petroleum Exploration and Production Technology (2020) 10:1317–1326
https://doi.org/10.1007/s13202-020-00835-2

ORIGINAL PAPER - PRODUCTION GEOLOGY

Determining the domain of in situ stress around Marun Oil Field's failed wells, SW Iran

Meisam Farsimadan[1] · Ali Naghi Dehghan[2] · Meysam Khodaei[3]

Received: 10 October 2019 / Accepted: 6 January 2020 / Published online: 31 January 2020
© The Author(s) 2020

Abstract

Accurate determination of the in situ stress domain in oil fields is of paramount importance in drilling, completion, and maintenance of wells and in petroleum geomechanics. Determination of the magnitude and direction of stresses induced by drilling around the wellbores is the first step in geomechanical studies and wellbore stability analyses. Regarding the importance of casing collapse problems in Marun Oil Field, as the first step of this investigation, geomechanical studies were conducted to determine the in situ stress domain in the failed wellbores. Using density measurements, the vertical stress (S_V) was estimated to be within the range of 85–90 MPa for all wellbores. To estimate maximum-horizontal-stress (S_{Hmax}) domain, Anderson's faulting theory and stress polygon were employed, and a value close to S_V was achieved. Also, minimum horizontal stress (S_{hmin}) was estimated using different approaches and was found to have the minimum in situ stress. Finally, the faulting regime of the areas was found to be normal/strike slip, where the stress values are close to each other due to salt lithology and high pore pressures in the Gachsaran Formation and thereby could be assumed as hydrostatic stresses.

Keywords In situ stress · Liner and casing collapse · Hydrostatic stress · Gachsaran Formation · Marun Oil Field

Introduction

In situ stress consists of three main components of vertical (S_V), minimum horizontal (S_{hmin}), and maximum horizontal (S_{Hmax}) stresses that are applied perpendicularly to rock at a certain depth. Drilling operation changes the equilibrium condition of in situ stress and creates a disturbed in situ stress state around the wellbore (Jaeger and Cook 1979). Such a stress disturbance around the wellbore wall creates some problems such as wellbore instability, tight hole, drilling-induced tensile fractures, breakout in the wellbore, and creep of salt layers toward the wellbore. Among the advantages of determining the in situ stress before and after drilling are the estimation of the optimum mud weight, optimum directional drilling trajectory to minimize risk level and lower maintenance costs, studying casing collapse and shear, wellbore stability analysis, designing a proper drilling bit for further drilling, selecting suitable casings, preventing sand production, selecting efficient strategies for well completion, and determining the optimum exploitation from the oil reservoir. Drilling-induced tensile fracture and breakouts are both the precursors of wellbore instability, which occur when the stress concentration on the wellbore wall is higher than the mechanical strength of the wellbore wall rock (Cao et al. 2016; Ju et al. 2018; Taherynia et al. 2016). Besides, drilling-induced tensile fracture and breakouts occur when the stress magnitude on the wellbore wall is larger than the tensile and compressive strengths of the rock, respectively (Bell and Gough 1979; Cao et al. 2016; Horn et al. 2016; Taherynia et al. 2016; Ju et al. 2018). Directions of drilling-induced tensile fracture and breakouts show the minimum horizontal stress (S_{hmin}) and maximum horizontal stress (S_{Hmax}), respectively (Bell and Gough 1979). Breakouts in wellbore wall can be detected and investigated using the image logs and caliper measurements while drilling-induced tensile fractures are only identified using the image logs (Peška and Zoback 1995; Brudy and Zoback 1993; Lund and Zoback 1999; Cao et al. 2016; Horn et al. 2016). Sedimentary rocks, in which oil field drilling occurs, are porous

✉ Ali Naghi Dehghan
a.dehghan@srbiau.ac.ir

[1] Department of Exploitation Geology, National Iranian South Oil Company (NISOC), Ahvaz, Iran

[2] Department of Mining Engineering, Science and Research Branch, Islamic Azad University, Tehran, Iran

[3] Department of Petroleum and Chemical Engineering, Science and Research Branch, Islamic Azad University, Tehran, Iran

and contain some fluids. Pore pressure is generally referred to as the fluid content of the formations. Normal pore pressure (P_{fn}) at a depth H is the weight of fluid column above that depth, which is defined as:

$$P_{fn} = \int_0^H \rho_f(z) g dz. \quad (1)$$

The fluid density for seawater is within the range of 1.03–1.07 g/cm^3. Thus, normal pore pressure indicates a ~ 10 MPa increase with a 1-km increase in depth (10 MPa/km or 0.45 psi/ft). In many important cases, the pore pressure deviates from the normal value and results in abnormal pore pressures (Fjaer et al. 2008).

Tests such as leak-off test (LOT), extended leak-off test (ELOT), micro-fracture test, and hydraulic fracturing can be applied to determine S_{hmin}. All these tests are carried out in situ at a certain depth. To perform these tests, the fluid pressure is increased at a certain depth until the fracture initiated and/or the pre-existing fracture reopened in the formation. The pressure recorded at the moment of fracture initiation presents the pressure needed to overcome rock strength, i.e., S_{hmin} (Jandakaew 2007; Dehghan et al. 2015a, b, 2016, 2017, Dehghan and Khodaei 2017).

One of the most frequently used methods for determining the domain of S_{Hmax} is to apply the stress polygon method. To determine the lower and upper bounds of S_{Hmax} using this method, we should have Biot coefficient, Poisson's ratio, wellbore azimuth, mud pressure difference, sliding friction, internal friction, pore pressure, uniaxial compressive strength (UCS), wellbore deviation, the azimuth of S_{Hmax}, and breakout width (W_{BO}). In this study, magnitude of in situ stress around the Marun Oil Field's failed wells was determined based on the field data and using the empirical equations and different methods.

Stress distribution in salt formations

Salt is one of the evaporite rocks, which is highly deformable with temperature and applied stresses. Stress state is highly complicated and varying in salt formations. Under the effect of in situ stress, this rock can show long-term viscoplastic and time-dependent (creep) behaviors (Jandakaew 2007). Allemandou and Dusseault (1996) conducted some triaxial creep tests on salt and identified the considerable role of octagonal shear stress and deviatoric stress on its creeping behavior. In this regard, creep tests were carried out under different temperature and pressure conditions on 10 core samples extracted from salts of the Gachsaran Formation, and their viscoplastic behavior was proved. Because of the role of evaporite cap rocks in hydrocarbon reservoirs and preventing oil escape, salt formations are suitable places for disposal of atomic waste and hydrocarbon storage (Winterle et al. 2012).

Due to the very low porosity and permeability of salt, an increase in the stress value is accompanied by its low compressibility and thus it starts to have a plastic movement. This phenomenon is attributed to the high Poisson's ratio of salts, according to which when a certain stress is applied to the salt, its stress state becomes almost hydrostatic due to its incapability to keep deviatoric stresses. Stress in salts reaches a relaxation state and finally turns into the hydrostatic state. However, by moving from the salt toward non-salt formations, the hydrostatic stress condition and magnitude are disturbed and the vertical and horizontal stress values are changed (Fredrich and Fossum 2002).

Since the salt rocks are viscous and flow slowly at all nonzero shear stress states, it can be assumed that $S_V = S_{Hmax} = S_{hmin} = \bar{\gamma} \cdot z$, where $\bar{\gamma}$ is the mean overburden bulk density. Isotropic stress state is seen only in viscous rocks and very soft mud. Assuming an isotropic stress state of salts, the horizontal stress would be almost equal to overburden. So, the term under-balance is commonly addressed in drilling of a salt formation, according to which mud pressure is less than the vertical stress (Dusseault et al. 2004).

Marun Oil Field and casing collapse phenomenon

Marun Oil Field was discovered in 1963 through the seismic exploration technique. This oil field neighbors Kupal field in the north, Aghajari in the east, and Ahvaz City in the northwest. This field is in the eastern part of huge Dezful subsidence. By now, about 400 oil wells have been drilled in this oil field. Marun Oil Field has a NW–SE direction from its western to central part and a NE–SW direction in its eastern part. The length and the width of this field are 65 km and 7 km, respectively. The distance between the reservoir crest and the deepest level of water–oil contact is the Asmari Formation is about 2000 m. The field has a fault with a similar name (i.e., Marun Fault), which is in the northwest of Aghajari Fault in Faulted Zagros Belt. The length of this NE–SE fault is about 50 km. The thrust fault has been thrust on the sediments of neighboring plain due to the performance of Marun Anticline. The evaporitic Gachsaran Formation consists of seven members with sequence of anhydrite, marl, and salt layers. The first member (the lowest one) which is made up of anhydrite is known as the cap rock of the Asmari carbonate reservoir, the most famous hydrocarbon reservoir in Iran.

According to the report of National Iranian South Oil Company (NISOC) and Schlumberger Oil Company in 2005 about the casing collapse problem in this field, 48 out of 267 wells (17.5%) drilled since the first oil production from this field

(1950) until 2005 had shown casing collapse problem (Rolf et al. 2006). Most of these failures have occurred in members 4–2 of the Gachsaran Formation, which consists of salt and associated a small portion of interlayers of marl and anhydrite with a varying thickness. The reason for the difference in thickness of this formation is the effect of tectonic of plastic materials that make the Gachsaran Formation. Considering the lithology and creep behavior with time, when the stress generated by the creeping movement of the Gachsaran salts applied on casing exceeds the collapse resistance of casing, it would definitely collapse (Rolf et al. 2006). Accordingly, it is necessary to determine in situ stress for the analysis and study of creep movements in the Gachsaran Formation Salts in the Marun Oil Field's failed wells. Marun Anticline has an NW–SE direction. As can be seen from the focal mechanism map of earthquakes in the southwestern part of Iran (Fig. 1), S_{Hmax} has an azimuth of 40–45°.

Determination of in situ stress in Marun 42, 130, and 133 wells

Determination of vertical stress (S_V)

Vertical stress (S_V) component is calculated from surface for the given depth using the density log of the wells (Fjaer et al. 2008):

$$S_V = \int_0^z \rho(z) g \mathrm{d}z \cong \bar{\rho} g z \tag{2}$$

where g is gravitational acceleration, $\bar{\rho}(z)$ is density at depth z, and $\bar{\rho}$ is the mean overburden density. The density of sedimentary rocks varies with a range of 2–3 g/cm^3, with the mean density being 2.5 g/cm^3. At higher depths (overburden) of the reservoir, for which density logs are

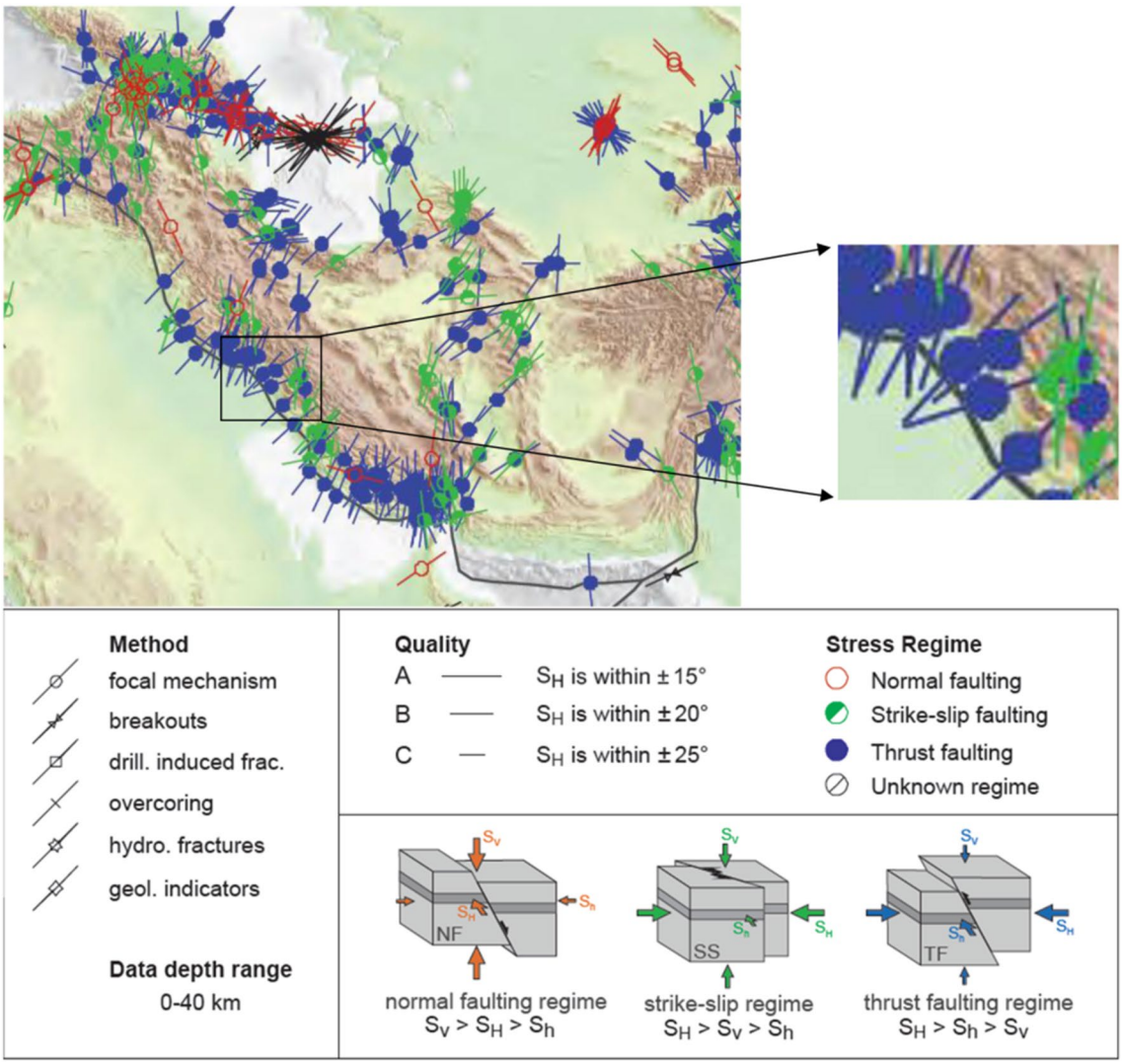

Fig. 1 Stress distribution map for Iran (general azimuth of S_{Hmax} based on earthquake focal data) (Rolf et al. 2006)

not available, density of rocks can be estimated for each lithology using geological graphic well logs or daily drilling reports. Since the reservoir is overlain by the Gachsaran Formation, density log was not available for estimating the S_V. However, as mentioned earlier, S_V can be estimated by averaging the densities of the existing lithologies (Zoback et al. 2003). Using the sonic logs and laboratory tests, the density of marl, anhydrite, and salt was estimated to be 2.55, 2.96, and 2.29 g/cm^3, respectively, which can be averaged to 2.6 g/cm^3. Accordingly, gradient of vertical stress in the Gachsaran Formation is 0.026 MPa/m. According to Eq. (2), S_V at failure depths in Marun 42, 130, and 133 wells was calculated as 85.3, 88.86, and 86.58 MPa, respectively. The failure depths for these three wells were 3281, 3418, and 3330 m, respectively.

Determination of minimum horizontal stress (S_{hmin})

Due to a lack of hydraulic fracturing and leak-off test data in the Gachsaran Formation of the Marun Oil Field, to calculate minimum horizontal stress, mud losses information of the formation was used. Thus, if the mud weight leads to the fracture initiation and/or reopening the pre-existing fractures in the formation, the total mud weight can be considered equivalent to the minimum horizontal stress (Zoback 2010; Ward and Andreassen 1997; Serdyukov et al. 2016; Wang and Mi 2016). Based on mud weight information in the daily drilling reports, pore pressure in member 4 of the Gachsaran Formation up to the cap rock (member 1) in the Marun Oil Field would be about 0.022 MPa/m. This value implies the presence of a large amount of saline water at this depth and thus overpressure of the Formation. In this way, pore pressure at failure depths of Marun 42, 130, and 133 wells was estimated to be 66.8, 73.44, and 71.55 MPa, respectively. Drilling in members 4–2 of the Gachsaran Formation in Marun 133 well shows that mud weight has increased up to 145 pcf, which was declined to 140 pcf by the mud loss of 22 barrels. The mud column weight pressure (i.e., well pressure at the depth of failure) was calculated to be 75.85 MPa. Since fracture gradient of the Gachsaran Formation was 0.024 MPa/m, due to the pre-existing fractures, the 145 pcf mud weight can initiate or propagate fracturing at the failure depth. Since the fracturing induced by mud weight increase up to the formation strength must occur along the direction of horizontal stress, by converting mud weight unit (pcf) to pressure unit (MPa), it is seen that mud column weight at

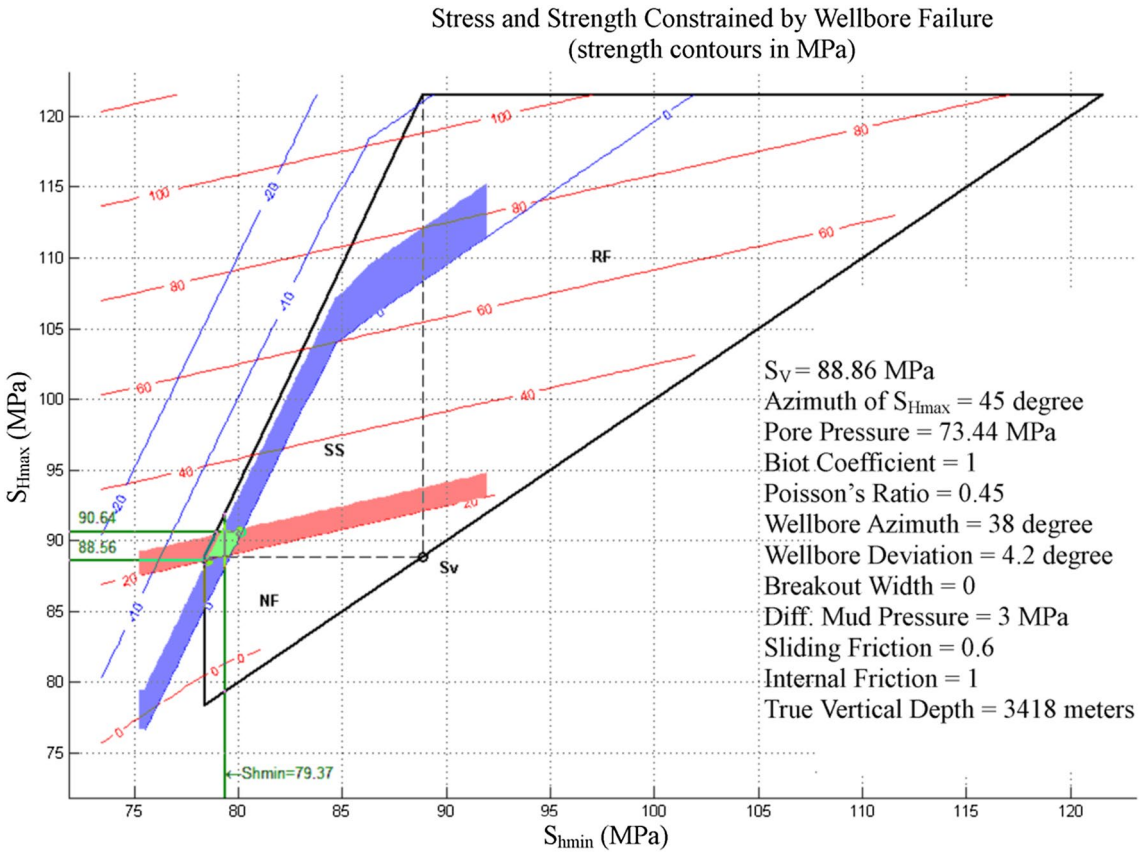

Fig. 2 Stress polygon based on the Mohr–Coulomb failure criterion for Marun 130 well

failure depth is almost equivalent to S_{hmin}. At failure depth of Marun 130 well, mud weight increased up to 150 pcf, by which the well pressure was increased to 80.54 MPa, while mud weight was declined to 146 pcf.

At failure depth of the Marun 42 well, mud weight was increased up to 145 pcf, which was reduced to 135 pcf. At this moment, well pressure at failure depth was 74.74 MPa.

Moreover, Eq. (3) proposed by Hubbert and Willis (1972) was also used in the present work. This relation was prepared by conducting a set of hydraulic fracturing tests and analyses. Later on, Zoback and Healy (1984) showed that the constant 0.5 is associated with friction faulting theory in which sliding friction coefficient can be considered as 0.6 (Zoback and Healy 1984). Thus, the S_{hmin} in the Marun 42, 130, and 133 wells was estimated to be 76.05, 81.15, and 79.06 MPa, respectively.

$$S_{hmin} = 0.5(S_V - P_p) + P_p. \quad (3)$$

Also, Breckels and van Eekelen (2008) used hydraulic fracturing results in several points and extracted a relationship between horizontal stress and depth. They incorporated the effect of the existing abnormal pressures in this equation and proposed Eqs. (4) and (5) (Fjaer et al. 2008). Also, Eaton (1969) proposed Eq. (6) for this purpose (Eaton 1969):

$$S_{hmin} = 0.0053H^{1.145} + 0.46(P_p - P_{fn}) \quad \text{For } H < 3500 \quad (4)$$

$$S_{hmin} = 0.026H - 31.7 + 0.46(P_p - P_{fn}) \quad \text{For } H > 3500 \quad (5)$$

$$S_{hmin} = \frac{\upsilon}{1-\upsilon}(S_V - P_p) + P_p \quad (6)$$

where H is depth (m), P_P is pore pressure (MPa), P_{fn} is normal pore pressure (with respect to a gradient of 10.5 MPa/km), and υ is a Poisson's ratio. Equations (4), (5), and (6) and stress polygon were used to estimate S_{hmin}.

Determination of maximum-horizontal-stress domain (S_{Hmax})

Although in salt cross sections S_V, S_{hmin}, and S_{Hmax} are considered to be equal, stress polygon method was employed to prove this assumption. In the Marun Oil field, in none of the damaged wells, there are no image logs in order to observe

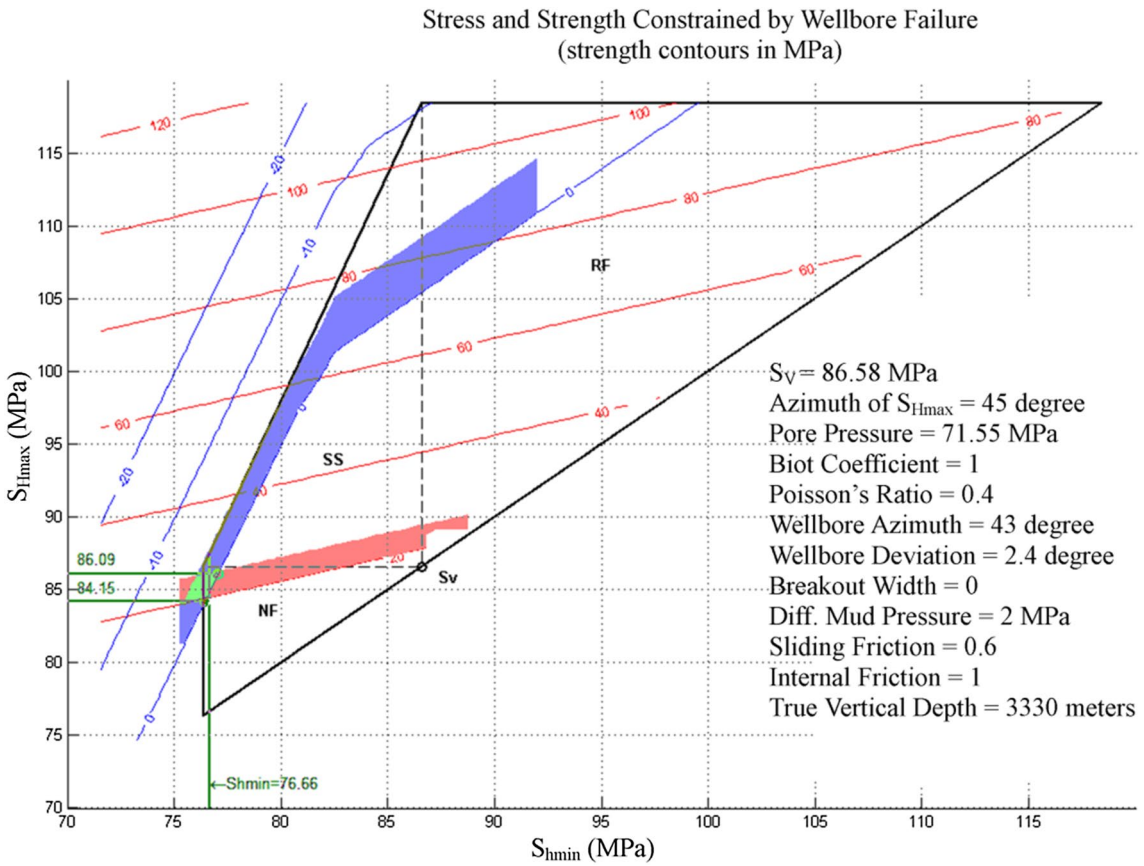

Fig. 3 Stress polygon based on the Mohr–Coulomb failure criterion for Marun 133 well

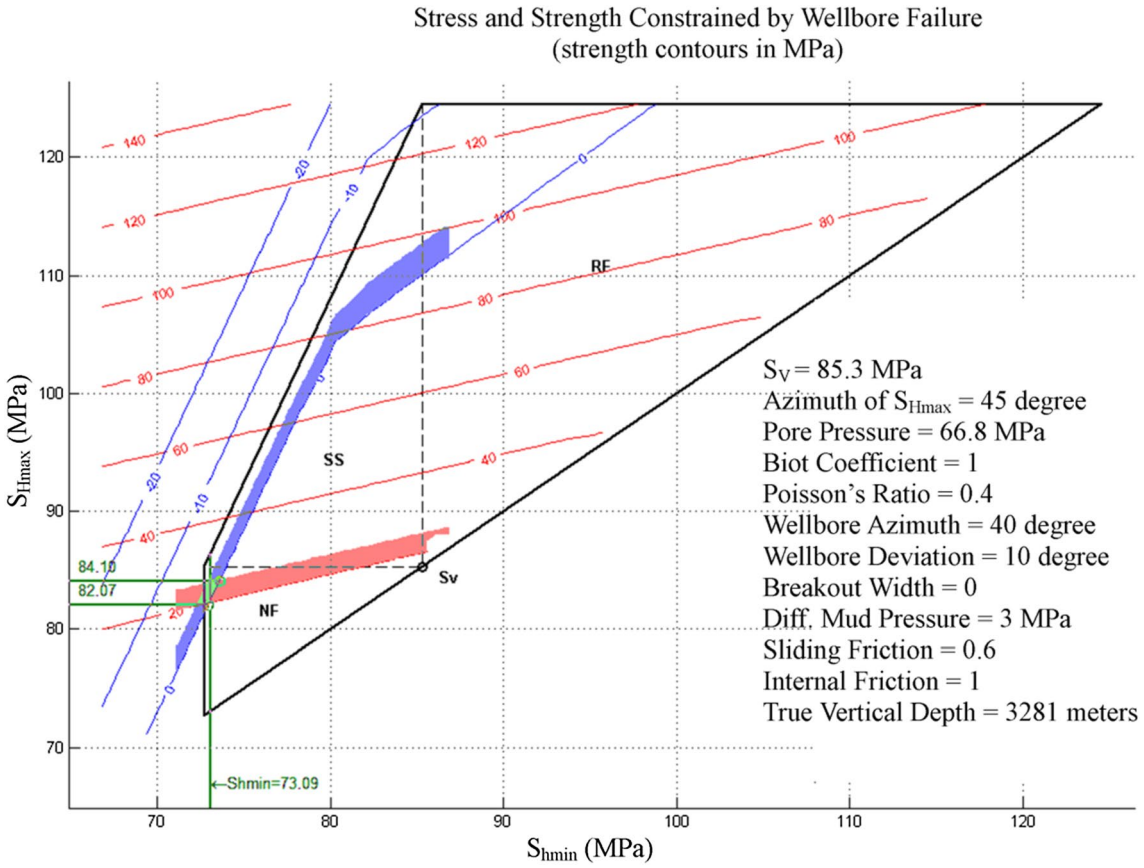

Fig. 4 Stress polygon based on the Mohr–Coulomb failure criterion for Marun 42 well

the drilling-induced tensile fractures, breakouts, or natural fractures in the wellbore.

Through the studies performed by petroleum geomechanical engineers around the world, it has been reported that drilling-induced tensile fractures and breakouts in wellbores are not related to lithology. In other words, these discontinuity planes can occur in any lithology in the well drilling path. In this regard, image well logs such as ultrasonic borehole imager (UBI) and fullbore formation microimager (FMI) can be used to identify and analyze the magnitude of S_{hmin} and S_{Hmax}. To determine S_{Hmax} using the stress polygon, it is necessary to have an azimuth of S_{Hmax} and breakout width (W_{BO}). Due to not having these two parameters, even having S_V, S_{hmin}, UCS, pore pressure, and well pressure, it is not possible to accurately estimate S_{Hmax} in these wells. Figures 2, 3, and 4 illustrate stress polygons obtained from the Mohr–Coulomb failure criterion for the Marun 130, 133, and 42 wells, respectively. This criterion is one of the shear failure criteria in rock engineering studies that can consider the low permeability of Gachsaran Formation.

In Figs. 2, 3, and 4, the information required for plotting stress polygons is presented. As can be seen, parameters including W_{BO} and the azimuth of S_{Hmax} are not available, which can both be extracted from image well log analyses. Based on earthquake focal data (Fig. 1), W_{BO} and azimuth of S_{Hmax} were considered to be 0° and 45°, respectively. The red parallel lines in the figure demonstrate contours of UCS, which were determined to be 22 MPa for the Gachsaran Formation salts. Moreover, the Poisson's ratio for this formation was estimated to be 0.45 (Farsimadan 2011). Steep blue parallel lines, on the other hand, illustrate contours of tensile strength, which are within the range of − 1 to − 2 MPa (Farsimadan 2011). By applying these two values and their intersection on stress polygon, we acquire an area (green shade) to calculate S_{hmin} as well as upper and lower bounds of S_{Hmax}. The red and blue shades also represent the range of compressive and tensile strengths for the Gachsaran Formation salts in the different wells, respectively (Figs. 2, 3, and 4).

Interpretation of obtained in situ stress

The in situ stress was determined for all depths of the Gachsaran Formation in Marun 42, 130, and 133 wells, and their gradients along with gradients of normal pore pressure, pore

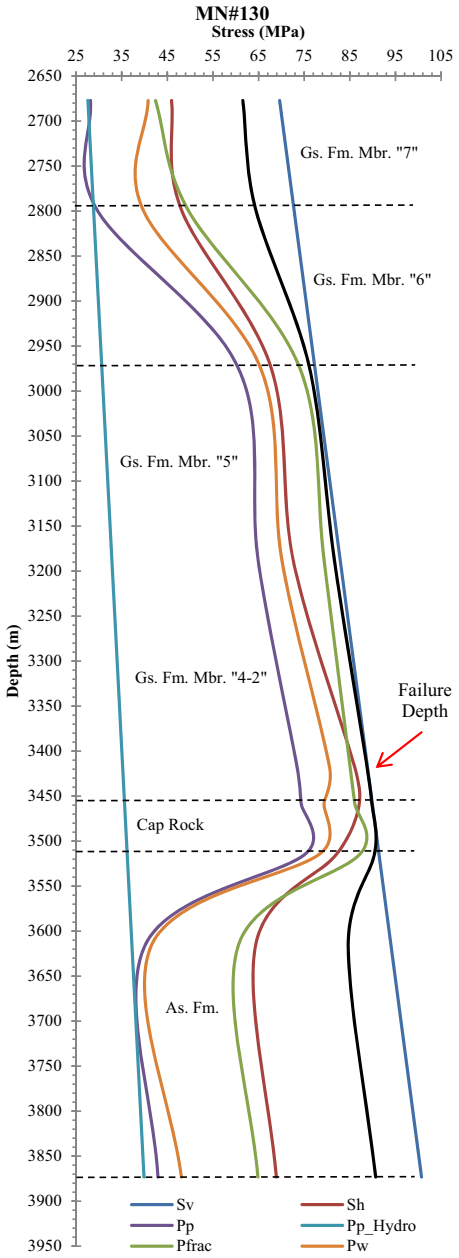

Fig. 5 In situ stress determined for Marun 130 well

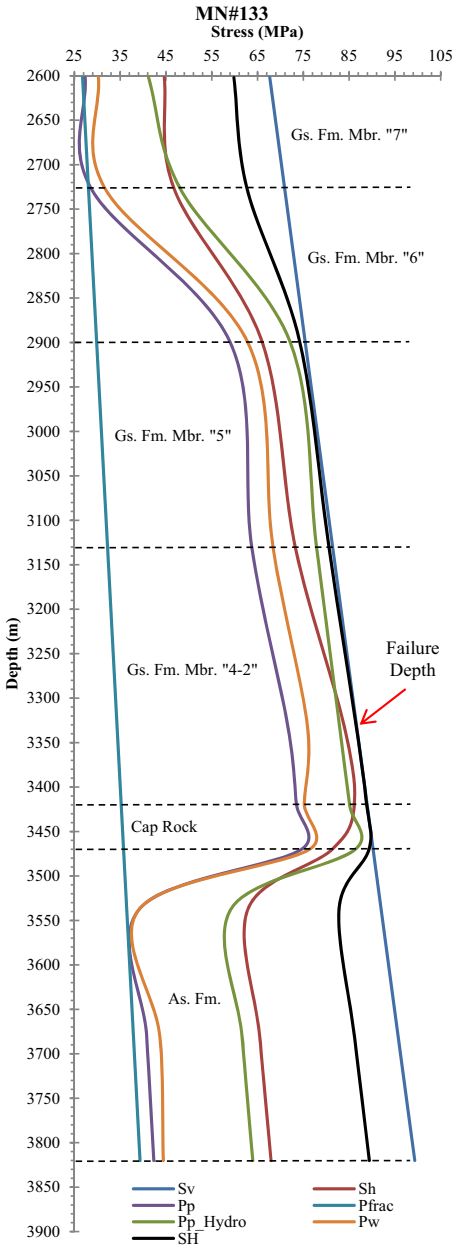

Fig. 6 In situ stress determined for Marun 133 well

pressure, and well pressure are presented in Figs. 5, 6, and 7. As can be seen in these figures, from a depth of 3000 m S_{Hmax} and S_V values become very close to each other, but they are both greater than S_{hmin}. One explanation for this observation is the high pore pressure that results in a convergence of stress in the stress polygon. The failure depths in these figures are denoted by arrows.

It is worth mentioning that the difference of S_{hmin}, S_{Hmax}, and S_V (for an assumed hydrostatic condition) for all three wells can be due to lack of complete information, the use of empirical equations, and more importantly the presence of marl and anhydrite layers at failure depths. Another noteworthy point in the failure zone is the increased S_{hmin} compared to fracture pressure gradient of the Gachsaran Formation. Table 1 summarizes the in situ stress results for Marun 42, 130, and 133 wells. The error values obtained for estimating

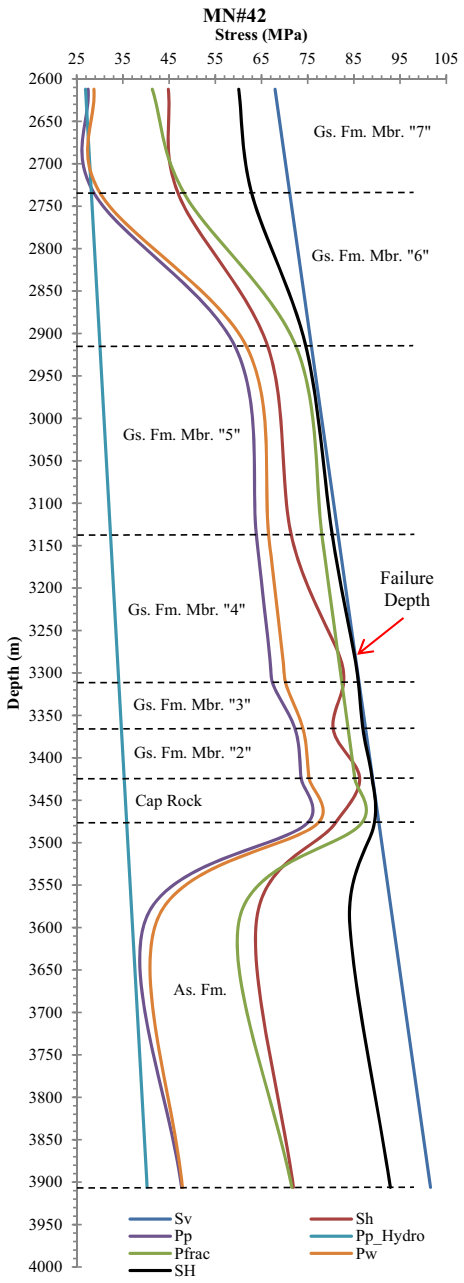

Fig. 7 In situ stress determined for Marun 42 well

S_{hmin} and S_{Hmax} relative to S_V by the different methods are shown with a +/− sign in Table 1.

Conclusion

The main conclusions of the present study can be summarized as follows:

1. At studied failure depths, due to the lithology of salt (and its viscoplasticity property) and high pore pressure, the values of estimated in situ stress are very close to each other, and the stress state can be considered as hydrostatic.
2. The S_{hmin} in Marun 130 well at failure depth obtained using the stress polygon was estimated as 79.37 MPa, which is slightly different from the 80.54 MPa stress estimated using the mud loss information. In addition, in this well, S_V is 88.86 MPa, while the lower and upper bounds of S_{Hmax} are, respectively, 88.56 and 90.64 MPa. Considering that S_V is smaller than the upper bound of S_{Hmax} but greater than its lower bound, the faulting stress regime can be considered as a combination of normal and strike slip modes.
3. S_{hmin} obtained using stress polygon for Marun 133 well at failure depth is 76.66 MPa, which is slightly different from the 75.85 MPa stress, obtained from mud loss of the formation. The upper and lower bounds of S_{Hmax} were, respectively, 84.15 and 86.09 MPa, while the S_V was 86.58 MPa. Since S_V is slightly larger than the upper bound of S_{Hmax}, it can be stated that the faulting regime is normal.
4. S_{hmin} obtained using stress polygon for Marun 42 well at failure depth is 73.09 MPa, which is slightly different from the 74.73 MPa stress, obtained from mud loss of the formation. Also, S_V at failure depth is 85.3 MPa that is slightly higher than the 84.1 MPa S_{Hmax} stress. Hence, a normal faulting mechanism can be considered for this well.
5. Based on the determined in situ stress, the overall faulting regime of the study area was determined to be normal/strike slip.
6. The S_V and S_{hmin} values at failure depth estimated using the relation proposed by Eaton (1969) are closer (because of the parameters used in this equation). Therefore, it is recommended for the estimation of S_{hmin}.

Table 1 The in situ stress results for Marun 42, 130, and 133 wells

Well no.	MN#130	MN#133	MN#42
Depth (m)	3418	3330	3281
P_p (MPa)	73.44	71.55	66.8
Max mud weight (pcf)	150	145	145
P_{frac} (MPa)	85.04	82.85	81.63
S_V (MPa)	88.86	86.58	85.3
S_{hmin} (Eaton) (MPa) /(error)	86.06/(−2.8)	83.84/(−2.74)	81.94/(−3.36)
S_{hmin} (excess of *P*w) (MPa)/(error)	80.54/(−8.32)	75.85/(−10.73)	74.74/(−10.56)
S_{hmin} (Hubbert and Willis) (MPa)/(error)	81.15/(−7.71)	79.06/(−7.52)	76.05/(−9.25)
S_{hmin} (Breckels and van Eekelen) (MPa)/(error)	76.16/(−12.7)	74.02/(−12.56)	71.12/(−14.18)
S_{hmin} (stress polygon) (MPa)/(error)	79.37/(−9.49)	76.66/(−9.92)	73.09/(−12.21)
S_{Hmax} (stress polygon) (MPa)/(error)	88.56–90.64 / (−0.3)–(+1.78)	84.15–86.09 / (−2.43)–(−0.49)	82.07–84.1 / (−3.23)–(−1.2)

Acknowledgements The authors would like to thank the National Iranian South Oil Company (NISOC) and Science and Research Branch, Islamic Azad University, for their cooperation in providing the needed data and instruments.

Open Access This article is licensed under a Creative Commons Attribution 4.0 International License, which permits use, sharing, adaptation, distribution and reproduction in any medium or format, as long as you give appropriate credit to the original author(s) and the source, provide a link to the Creative Commons licence, and indicate if changes were made. The images or other third party material in this article are included in the article's Creative Commons licence, unless indicated otherwise in a credit line to the material. If material is not included in the article's Creative Commons licence and your intended use is not permitted by statutory regulation or exceeds the permitted use, you will need to obtain permission directly from the copyright holder. To view a copy of this licence, visit http://creativecommons.org/licenses/by/4.0/.

References

Allemandou X, Dusseault MB (1996) Procedures for cyclic creep testing of salt rock, results and discussion. Ser Rock Soil Mech 20:207–220

Bell JS, Gough DI (1979) Northeast-southwest compressive stress in Alberta evidence from oil wells. Earth Planet Sci Lett 45(2):475

Brudy M, Zoback MD (1993) Compressive and tensile failure of boreholes arbitrarily-inclined to principal stress axes: application to the KTB boreholes, Germany. Int Journal Rock Mech Min Sci Geomech Abstr 30(7):1035–1038

Cao W, Deng J, Yu B, Tan Q, Liu W, Li Y, Gao J (2016) A revised method of in-situ stress determination from drilling-induced fractures: a case study of high temperature and low permeability formation drilling. In: 50th US rock mechanics/geomechanics symposium. American Rock Mechanics Association

Dehghan AN, Khodaei M (2017) The experimental comparative study of the effect of pre-existing fracture on hydraulic fracture propagation under true tri-axial stresses. J Pet Res 27(4):71–80

Dehghan AN, Goshtasbi K, Ahangari K, Jin Y (2015a) Experimental investigation of hydraulic fracture propagation in fractured blocks. Bull Eng Geol Environ 74(3):887–895

Dehghan AN, Goshtasbi K, Ahangari K, Jin Y (2015b) The effect of natural fracture dip and strike on hydraulic fracture propagation. Int J Rock Mech Min Sci 75:210–215

Dehghan AN, Goshtasbi K, Ahangari K, Jin Y (2016) Mechanism of fracture initiation and propagation using a tri-axial hydraulic fracturing test system in naturally fractured reservoirs. Eur J Environ Civil Eng 20(5):560–585

Dehghan AN, Goshtasbi K, Ahangari K, Jin Y, Bahmani A (2017) 3D numerical modeling of the propagation of hydraulic fracture at its intersection with natural (pre-existing) fracture. Rock Mech Rock Eng 50(2):367–386

Dusseault MB, Maury V, Sanfilippo F, Santarelli FJ (2004) Drilling through salt: constitutive behavior and drilling strategies. In: Gulf rocks 2004, the 6th North America rock mechanics symposium (NARMS). American Rock Mechanics Association

Eaton BA (1969) Fracture gradient prediction and its application in oilfield operations. J Petrol Technol 21(10):1–353

Farsimadan M (2011) Review of rock creep influence on casing collapse in Marun Oil Field (Master's thesis). Science and Research Branch, Islamic Azad University, Tehran, Iran

Fjaer E, Holt RM, Raaen AM, Risnes R, Horsrud P (2008) Petroleum related rock mechanics, vol 53. Elsevier, Dordrecht

Fredrich JT, Fossum AF (2002) Large-scale three-dimensional geomechanical modeling of reservoirs: examples from California and the deepwater Gulf of Mexico. Oil Gas Sci Technol 57(5):423–431

Horn H, Saasen A, Skogvang A (2016) A method for determination of stress and fatigue in risers and wellheads. In: IADC/SPE drilling conference and exhibition. Society of Petroleum Engineers

Hubbert MK, Willis DG (1972) Mechanics of hydraulic fracturing

Jaeger JC, Cook NGW (1979) Fundamentals of rock mechanics. Chapman & Hall, New York

Jandakaew M (2007) Stress-path dependency of rock salt. In: Proceeding of the first Thailand symposium on rock mechanics. Suranaree University of Technology, Greenery Resort, Khao Yai, Nakhon Ratchasima, pp 171–188

Ju W, Shen J, Qin Y, Meng S, Li C, Li G, Yang G (2018) In-situ stress distribution and coalbed methane reservoir permeability in the Linxing area, eastern Ordos Basin, China. Front Earth Sci 12(3):545–554

Lund B, Zoback MD (1999) Orientation and magnitude of in situ stress to 6.5 km depth in the baltic shield. Int J Rock Mech Min Sci 36(2):169–190

Peška P, Zoback MD (1995) Compressive and tensile failure of inclined well bores and determination of in situ stress and rock strength. J Geophys Res Solid Earth 100(B7):12791–12811

Rolf B, Mohammed W, Mohsen P (2006) A preliminary study of casing collapse in Iran Hydroquest Report. Schlumberger Oil Company, Houston

Serdyukov SV, Kurlenya MV, Patutin AV (2016) Hydraulic fracturing for in-situ stress measurement. J Min Sci 52(6):1031–1038

Taherynia MH, Aghda SMF, Fahimifar A (2016) In-situ stress state and tectonic regime in different depths of earth crust. Geotech Geol Eng 34(2):679–687

Wang Y, Mi Q (2016) In-situ stress perturbations and determinations near a fault and their impacts on hydraulic fracturing design. In: SPE Asia Pacific hydraulic fracturing conference. Society of Petroleum Engineers

Ward CD, Andreassen E (1997) Pressure while drilling data improves reservoir drilling performance. In: SPE/IADC drilling conference. Society of Petroleum Engineers

Winterle J, Ofoegbu G, Pabalan R, Manepally C, Mintz T, Pearcy E, Fedors R (2012) Geologic disposal of high-level radioactive waste in salt formations. Contract NRC-02-07-006. US Nuclear Regulatory Commission

Zoback MD (2010) Reservoir geomechanics. Cambridge University Press, Cambridge

Zoback MD, Healy JH (1984) Friction, faulting, and "in-situ" stresses. Ann Geophys 2:689–698

Zoback MD, Barton CA, Brudy M, Castillo DA, Finkbeiner T, Grollimund BR, Wiprut DJ (2003) Determination of stress orientation and magnitude in deep wells. Int J Rock Mech Min Sci 40(7–8):1049–1076

Publisher's Note Springer Nature remains neutral with regard to jurisdictional claims in published maps and institutional affiliations.